Materials Research Proceedings 54 (2025) 355-362 https://doi.org/10.21741/9781644903599-39

Experimental investigation to reduce knit line effects in C-SMC

Marcel Olma[1,a *], Nils Meyer[2,b], Sergej Ilinzeer[3,c], Florian Wittemann[1,d], Constantin Krauß[1,e], Luise Kärger[1,f]

[1]Rintheimer Queralle 2, 76131 Karlsruhe, Karlsruher Institute of Technology, Germany

[2]Am Technologiezentrum 8, 86159 Augsburg, University of Augsburg, Germany

[3]Joseph-von-Fraunhofer-Straße 7, 76327 Pfinztal, Fraunhofer Institute for Chemical Technology ICT, Germany

[a]marcel.olma@kit.edu, [b]nils.meyer@uni-a.de, [c]sergej.ilinzeer@ict.fraunhofer.de, [d]florian.wittemann@kit.edu, [e]constantin.krauss@kit.edu, [f]luise.kaerger@kit.edu

Keywords: Sheet Molding Compound, Compression Molding, Knit Lines, Carbon Fiber, Tension Test

Abstract. The integration of structural features, such as metallic inserts, into carbon fiber-reinforced sheet molding compound (C-SMC) components can be achieved through overmolding. The complexity of the structure and the presence of integrated metallic inserts, however, result in the formation of knit lines, which can lead to a reduction of structural performance. In a conventional SMC initial stack concept (Concept A), the initial stack is placed in the center of the mold. In this work, a new initial stack concept is investigated (Concept B), where the metallic inserts are wrapped in SMC. An experimental comparison of the two different insert concepts demonstrates how the position of the initial stacks of C-SMC can be optimized to enhance the structural performance.

Introduction

Carbon fiber-reinforced sheet molding compounds (C-SMC) are utilized in the fabrication of lightweight structural components. The complexity of components manufactured from C-SMC is increasing in terms of their geometry. Structural components are produced for automotive and aircraft sectors [1, 2, 3]. The installation of C-SMC components may require the integration of connecting elements, such as metallic inserts. In addition to the crucial factor of reducing the weight of the component to a minimum, the strength of the bond between the insert and the C-SMC is also an important aspect to consider in order to exploit the full potential of the material. One method for integrating the inserts into the C-SMC involves the preliminary drilling of holes through the initial stacks to create the necessary space [4]. However, it is not always possible to work with complete molding coverage in C-SMC, especially in complex geometries. Another approach to include inserts without knit lines is a combination of foam and SMC [2]. In accordance with the current state of technology for pure SMC, the inserts are overmolded.

During the compression molding process, the metallic inserts get surrounded by C-SMC, which has the potential to form a splitting flow front. It has been observed that these flow fronts often form a knit line when they merge with one another [5]. A knit line forms a resin-rich area of a composite component with a reduced fiber volume fraction. Cranston and Reitz [6] showed a significant reduction of the tensile strength if knit lines occur in a flat geometry compared to a knit line free section. Martulli et al. [7] studied five different initial stack placements for a thick-walled part with two inserts. The publication states that the initial stack placement is more critical to the bending load applied than the pressure and temperature process parameters during compression molding.

Materials Research Proceedings 54 (2025) 355-362 https://doi.org/10.21741/9781644903599-39

The influence of the knit lines is investigated in our experimental study by producing components with two different variants of initial stack positions and then testing them destructively under uniaxial tension. For the experimental study, a symmetrical geometry with two metallic inserts was designed, manufactured, and tested as a demonstrator component. The results of the experimental study reveal the influence of the initial stack position. They can also be used to validate SMC process simulations on mesoscale, such as the direct bundle simulation approach proposed by Meyer et al. [8, 9, 10].

Materials and Geometry

The C-SMC material under investigation is based on a vinyl ester matrix with the composition shown in Table 1. The fiber volume content is approximately 40 %, which corresponds to a fiber mass content of 50 % with the matrix density $\rho_{\mathrm{m}} = 1200\ \mathrm{kg/m^3}$ and the density of the carbon fibers $\rho_{\mathrm{f}} = 1800\ \mathrm{kg/m^3}$.

Table 1 – Composition of the matrix.

Component	Trade name	Quantity	Mass fraction in %
Vinylester resin	CFOP-8200TD	100 parts	85.2
Dispersing aid	BYK 9076	3 parts	2.6
Inhibitor	pBQ	0.3 parts	0.3
Peroxide, initiator	TBPB	1.5 parts	1.2
Release agent	Zincum 5	4 parts	3.4
Magnesium oxide	Luvatol MK 35 NV	8.57 parts	7.3

The geometry of the component is shown in Fig. 1. The component dimensions are 155 mm in length, 35 mm in width, and 18 mm in height. The aluminum inserts are positioned at a center distance of 120 mm from each other and have an inner diameter of 20 mm with a wall thickness of 2.5 mm. The height of the inserts is 17 mm leaving a safety margin of 1 mm during molding. This safety margin ensures that only the C-SMC is compressed and that the inserts are not subjected to any forces from the upper tool. The C-SMC is 5 mm thick between the insert and the outer edge of the part. The component geometry allows force transition on the inserts in a uniaxial tensile testing machine.

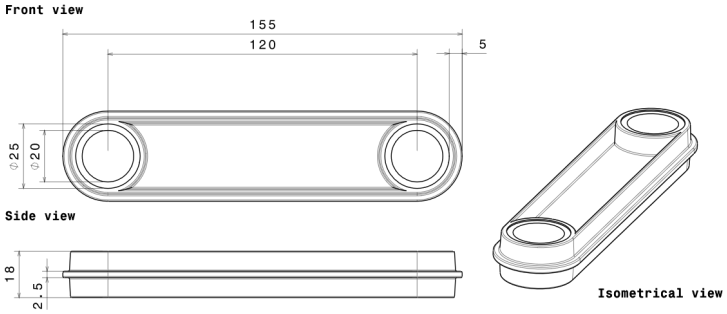

Figure 1 – Front, side and isometric view of the geometry of the tension rod (dimensions in millimeter).

Initial stack placements

Two concepts (A and B) are designed, manufactured, tested, and compared. In Concept A, a cuboid stack is positioned centrally within the inner cavity between the inserts. In Concept B, the central stack is thinner and complemented by wrapped C-SMC around the metallic inserts. In order to maintain the total mass of the C-SMC at a constant level for both concepts, the height of the stack in Concept B is reduced. A summary of the stack dimensions is provided in Table 2.

Table 2 – Stack dimensions of Concept A and Concept B.

	Unit	Concept A	Concept B
Base area stack	mm^2	90 × 33	stack: 90 × 33, winding: 85 × 18
Number of layers	-	6	stack: 5, winding: 2
height	mm	9-10	stack: 8-9, winding: 2-4
Mass	g	36 ±5.55 %	stack: 30 ±3.33 %, winding: 6

In Fig. 2, both concepts are displayed, where the right section of Concept B is enlarged to highlight the rolled stack. In the initial position, the cuboid stack in both concepts is in contact with the lateral wall surfaces, so material flows predominantly in the x-direction along the component and in the thickness direction of the component. The winding stack is manually positioned around the metallic insert and placed into the mold prior to the large cuboid stack being inserted. During the wrapping process, a pressure force is applied to the rolled stack on the insert in order to utilize the adhesive effect of the SMC and ensure adequate adhesion of the stack to the insert.

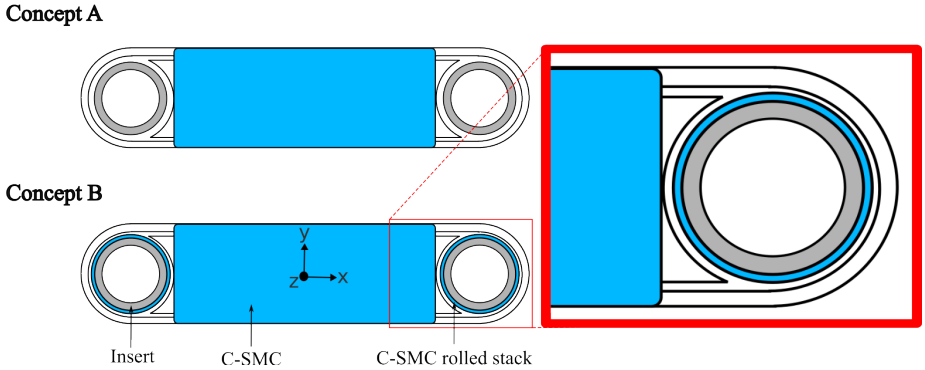

Figure 2 – Top view of the initial stack placement of Concept A and Concept B. The right section of Concept B is enlarged to highlight the rolled stack.

Manufacturing of the samples

Fig. 3 shows the bottom tool with the SMC stacks of the two initial-charge concepts A and B. Compression molding was carried out on a Dieffenbacher press. Both top and bottom molds are temperature-controlled to a constant temperature of 140 °C for manufacturing Concept A and Concept B. An internal press controller regulates the closing of the press according to the speed profile in Table 3 and up to a maximum of 200 kN, which corresponds to 66.6 kN per component, assuming ideal loading conditions.

If the applied force of the press exceeds 200 kN, this force is kept constant for 3 minutes to ensure complete curing.

Table 3 – Velocity profile of the top mold with linear interpolation between different mold openings.

Mold opening in mm	Velocity in mm/s
50	15
30	10
10	5

The molds are designed with three identical cavities, allowing for the production of three parts with each press cycle. To enhance the traceability of the samples, a nomenclature system has been implemented, whereby each sample is assigned a unique name code. The designations "A" and “B” represent the two initial-charge concepts. This is followed by the pressing cycle, with the subsequent number indicating the cavity utilized. For instance, "A2-1" signifies a sample with

initial-charge Concept A, produced in the second cycle within the first of the three cavities. An overview of all tested samples is shown in the results section in Fig. 7.

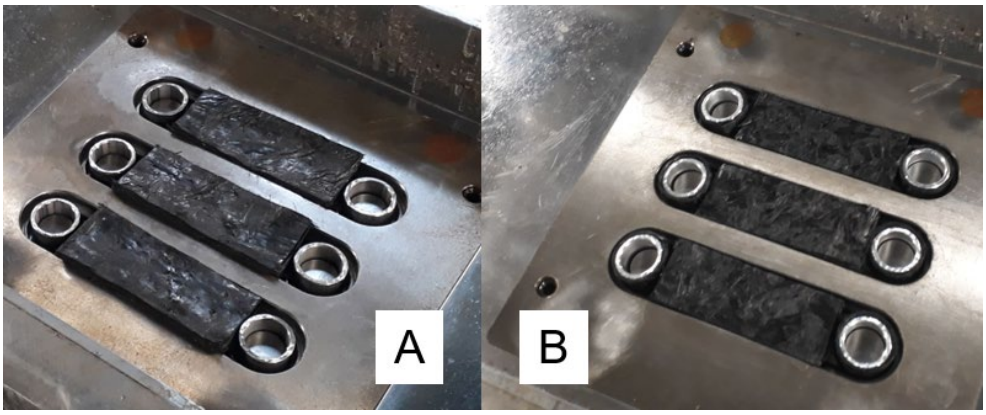

Figure 3 – Bottom mold with three identical cavities with initial SMC stacks of Concept A (left) and Concept B (right).

Testing

The tests are conducted on a *Hegewald & Peschke inspect 50 table* uniaxial tension testing machine. A clamping mechanism with two metrical screws is used to secure the component between the inserts on the testing machine, cf. Fig. 4. The original configuration was utilized for the assessment of 3D filament winding structures [11]. The lower end of the clamping is translationally fixed in all spatial directions. The upper insert is pulled upwards at a constant speed of 5 mm/min.

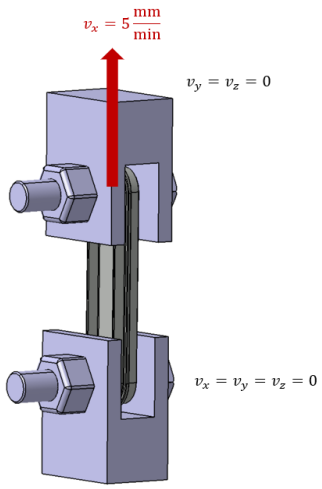

Figure 4 – Schematic 3D representation of a sample attached to the test rig using screws and loaded under tension. The boundary conditions are specified by the velocities.

Results

Fig. 5 shows the force-displacement curves for the entire measurement period (left) and for the first millimeter of displacement (right) for Concept A (green) and Concept B (red). A maximum displacement of 20 mm is applied, which results in a maximum test time of four minutes per sample. Concept B features greater maximum forces, with six out of seven samples reaching higher maximum forces than the strongest sample of Concept A.

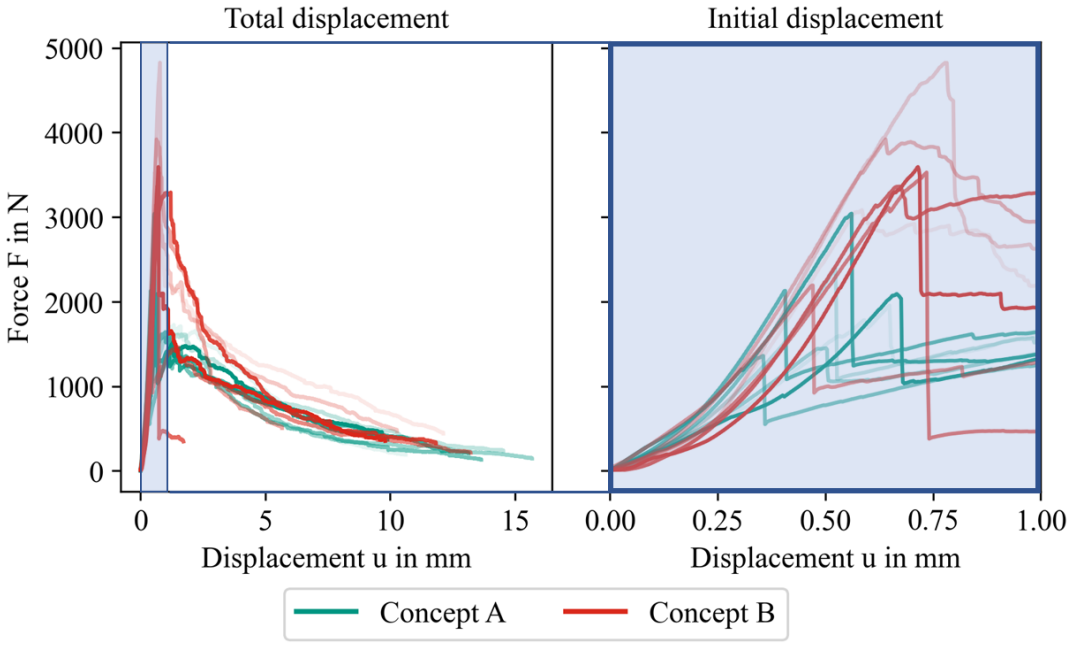

Figure 5 – Force-displacement curves for the total displacement (left) and for the first millimeter of displacement (right). Concept B exhibits higher initial forces and more scatter compared to Concept A. Coloring corresponds to Fig. 6.

An overview of the maximum forces is shown in Fig. 6.

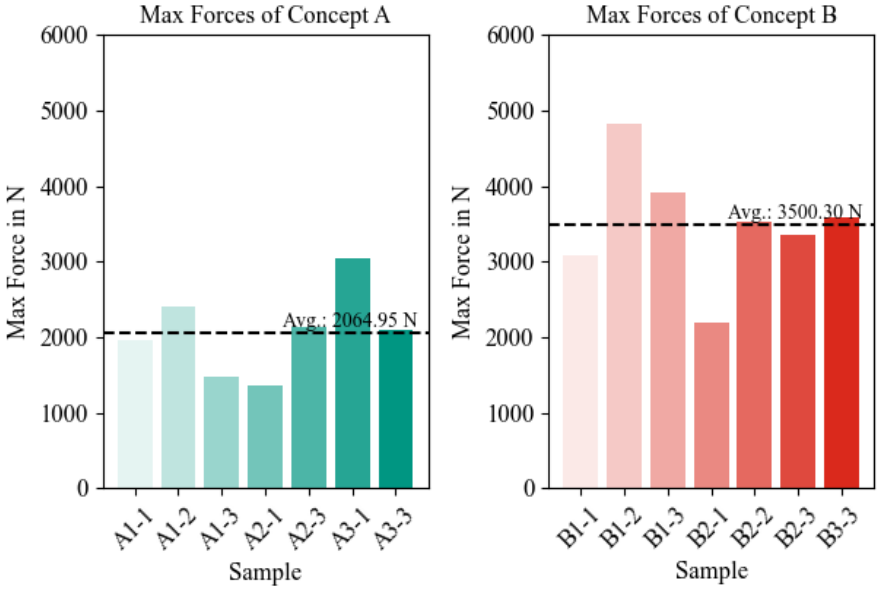

Figure 6 – Maximum forces of all tested samples and their averages for Concept A and Concept B.

The maximum forces of the specimens of the Concept A are reached at smaller displacements. The failure point is reached in the first phase of deformation, as evidenced by the abrupt decline in force following the maximum force. If comparing the average values of the maximum force, there is an increase of 69% from 2065 N (with standard deviation of $\sigma = 524.51$ N) for components manufactured using Concept A to 3500 N ($\sigma = 740.70$ N) for components manufactured using Concept B. A one-sided t-test at a significance level of α=0.05 with 10 degrees

of freedom shows that the increase in mean force values from Concept B to Concept A is statistically significant.

In addition to the force-displacement curves, the samples can also be analyzed visually. All 14 test components are inspected after the test for fracture patterns and labeled with their specimen number, cf. Fig. 7.

Figure 7 – All 14 test components after testing, marked with their component numbers (white), position of fracture at debonding between insert and C-SMC (green) and between rolled and flowed C-SMC (purple).

If a component fails, it is observed for both configurations that only one insert fails, while the other remains in place. All inserts remain in contact with the component at the end of the test. In the event of a failure of the bond between the insert and the C-SMC, a fracture may occur in the flank on either the upper or lower side, or in both sides in both concepts shown with green markers in Fig. 7. In Concept B, the bond between the insert and the rolled stack, as well as between the rolled stack and the remaining C-SMC material, can be subjected to detailed examination. The detachment of the insert from the wrapping as well as the detachment from the wrapping to the formed cuboid stack can be observed in samples B1-1, B2-1 and B1-2, as illustrated in Fig. 7 with the purple boxes. It is difficult to draw a conclusion as these are the samples with the lowest and also the highest maximum forces.

For both initial stack Concepts A and B, the knit lines are formed during manufacturing in the area where the flow fronts meet. However, the knit line in Concept B is smaller than in Concept A due to the rolled C-SMC around the inserts, cf. Fig. 8. In the tensile tests, the knit lines of both configurations are subjected to tension in circumferential direction, superposed by compression in transverse direction. By comparing the fracture surfaces of the two concepts, the edge of

Concept A appears smoother than that of Concept B. In Concept B, the fibers are aligned in the circumferential direction due to the wrapping. Thus, fiber breakage and fiber pull-out occur, increasing the tensile strength and influencing the form of the fracture surface. In Concept A, the fibers are oriented more or less parallel to the knit line shown in Fig. 8, thus transverse to the tensile stresses. These transversally oriented fibers cannot withstand as high tension stresses as the circumferentially oriented fibers, and thus the C-SMC is therefore more likely to fail. When comparing the failure of the inserts, Martulli et al. [7] come to similar conclusions: the smooth fracture surfaces indicate matrix failure, and the protruding fibers indicate fiber failure.

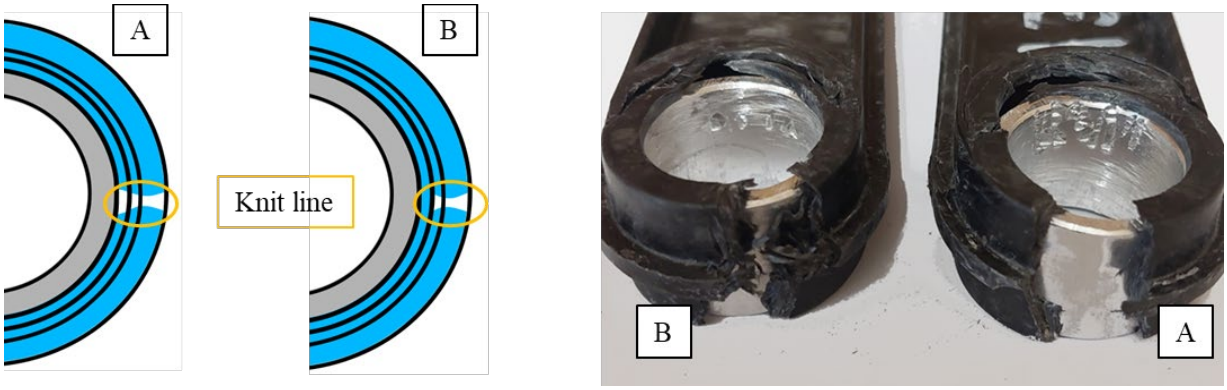

Figure 8 – Location of the knit lines (left) and the fracture on the knit line (right).

Conclusion and outlook

In this work, two initial-stack strategies were investigated experimentally to reduce the adverse effect of knit lines and improve the structural performance in C-SMC, which was validated through uniaxial tension tests. Components with two metallic inserts were fabricated such that two flow fronts meet and form a knit line. Through a new initial stacking concept with two C-SMC layers wrapped around the metallic inserts, the occurrence of knit lines could be minimized, resulting in greater load-bearing capacity on average. In future work, a mesoscopic process simulation approach will be enhanced to model the wrapped initial stack configuration and can then be validated against the manufacturing data of the investigated stack configurations. Further experiments are planned on the splitting behavior of the carbon fiber bundles during the compression molding process.

Acknowledgements

The research was initiated as part of the MANIFEST ZIM project, funded by the German Federal Ministry for Economic Affairs and Climate Action (BMWK). We would like to thank the BMWK also for funding the EcoDynamic SMC project, which allowed us to continue the work. The testing of the samples took place at the ICT under the guidance of Jonathan Haas which is gratefully acknowledged.

References

[1] M. Fette, M. Hentschel, F. Köhler, J. Wulfsberg, and A. Herrmann, ‘Automated and Cost-efficient Production of Hybrid Sheet Moulding Compound Aircraft Components’, *Procedia Manuf.*, vol. 6, pp. 132–139, 2016. https://doi.org/10.1016/j.promfg.2016.11.017.

[2] J. Buck, M. Mayer, and M. Fette, ‘Experimental Investigation of Inserts in SMC Foam Sandwich Structures for Aircraft Interior Applications’, in *Production at the leading edge of technology*, J. P. Wulfsberg, W. Hintze, and B.-A. Behrens, Eds., Berlin, Heidelberg: Springer Berlin Heidelberg, 2019, pp. 169–178. https://doi.org/10.1007/978-3-662-60417-5_17.

[3] V. Romanenko, M. Duhovic, D. Schommer, J. Hausmann, and J. Eschl, ‘Advanced process simulation of compression molded carbon fiber sheet molding compound (C-SMC) parts

in automotive series applications', *Compos. Part Appl. Sci. Manuf.*, vol. 157, p. 106924, Jun. 2022. https://doi.org/10.1016/j.compositesa.2022.106924.

[4] S. V. Hoa, A. Di Maria, and D. Feldman, 'Inserts for fastening sheet molding compounds', *Compos. Struct.*, vol. 8, no. 4, pp. 293–309, Jan. 1987. https://doi.org/10.1016/0263-8223(87)90021-3.

[5] P. S. Stelzer, U. Cakmak, L. Eisner, L. K. Doppelbauer, I. Kállai, G. Schweizer, H. K. Prammer, and Z. Major, 'Experimental feasibility and environmental impacts of compression molded discontinuous carbon fiber composites with opportunities for circular economy', *Compos. Part B Eng.*, vol. 234, p. 109638, Apr. 2022. https://doi.org/10.1016/j.compositesb.2022.109638.

[6] J. J. Cranston and J. A. Reitz, 'SMC Molding Techniques for Optimized Mechanical Properties in Structural Applications', *Polym.-Plast. Technol. Eng.*, vol. 15, no. 2, pp. 97–114, Jan. 1980. https://doi.org/10.1080/03602558008070007.

[7] L. M. Martulli, T. Creemers, E. Schöberl, N. Hale, M. Kerschbaum, S. V. Lomov, and Y. Swolfs, 'A thick-walled sheet moulding compound automotive component: Manufacturing and performance', *Compos. Part Appl. Sci. Manuf.*, vol. 128, p. 105688, Jan. 2020. https://doi.org/10.1016/j.compositesa.2019.105688.

[8] N. Meyer, 'Mesoscale simulation of the mold filling process of Sheet Molding Compound', Doctoral Thesis, Karlsruhe Institute of Technology (KIT), Karlsruhe, 2021. [Online]. Available: DOI: 10.5445/IR/1000138778

[9] N. Meyer, S. Ilinzeer, A. N. Hrymak, F. Henning, and L. Kärger, 'Non-isothermal direct bundle simulation of SMC compression molding with a non-Newtonian compressible matrix', *J. Non-Newton. Fluid Mech.*, vol. 310, p. 104940, Dec. 2022. https://doi.org/10.1016/j.jnnfm.2022.104940.

[10] N. Meyer, L. Schöttl, L. Bretz, A. N. Hrymak, and L. Kärger, 'Direct Bundle Simulation approach for the compression molding process of Sheet Molding Compound', *Compos. Part Appl. Sci. Manuf.*, vol. 132, p. 105809, Jan. 2020. https://doi.org/10.1016/j.compositesa.2020.105809.

[11] J. Haas, D. Aberle, A. Krüger, B. Beck, P. Eyerer, L. Kärger, and F. Henning, 'Systematic Approach for Finite Element Analysis of Thermoplastic Impregnated 3D Filament Winding Structures—Advancements and Validation', *J. Compos. Sci.*, vol. 6, no. 3, p. 98, Mar. 2022. https://doi.org/10.3390/jcs6030098.